Fermilab Muon g-2 final result

Alberto Lusiani
Scuola Normale Superiore and INFN, sezione di Pisa
for the FNAL Muon g-2 collaboration

8th Plenary workshop of the Muon g-2 Theory Initiative
8–12 Sept 2025, IJCLab, Orsay

PRL publication dated 2 Sep 2025

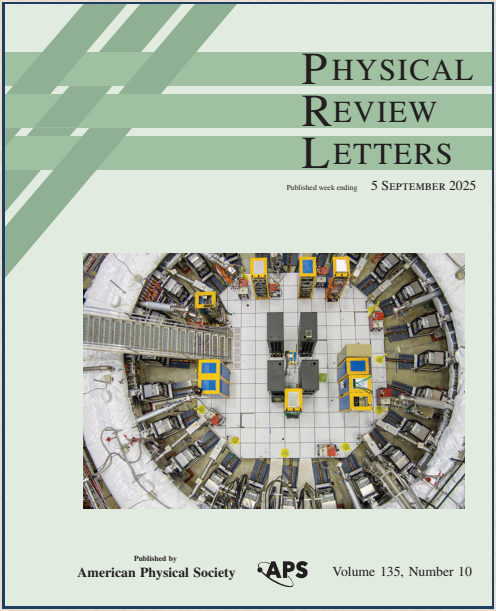

PRL Editor's suggestion

04/09/2025, 13:35 Physical Review Letters - Volume 135 Issue 10

HIGHLIGHTED ARTICLES

FEATURED IN PHYSICS EDITORS' SUGGESTION

Measurement of the Positive Muon Anomalous Magnetic Moment to 127 ppb

D. P. Aguillard *et al.* (Muon $g-2$ Collaboration)

Phys. Rev. Lett. **135**, 101802 (2025) - Published 2 September, 2025

The final results from the Muon $g-2$ experiment agree with the latest predictions of muon's magnetic properties—letting down hopes that the particle would upset the standard model's applecart.

PRL 135 (2025) 101802

Data sample over 6 years (analyzed positrons)

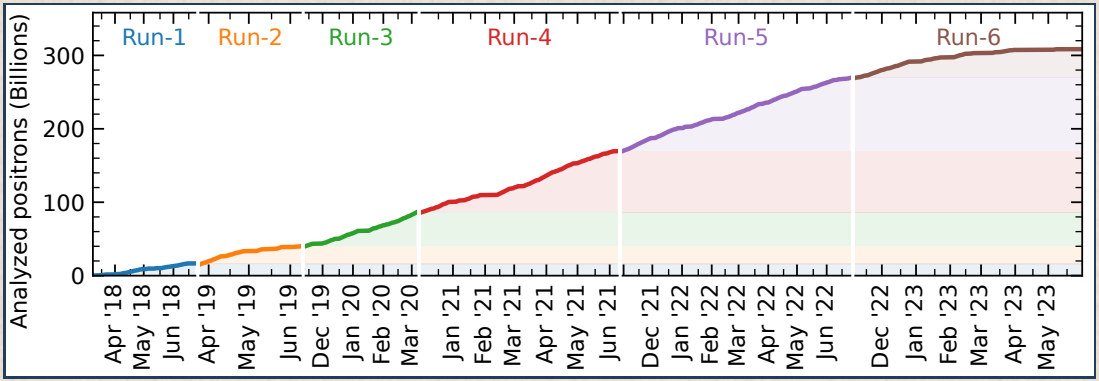

- April 2021: Run-1
- August 2023: Run-2/3 (and combination with Run-1)
- June 2025: Run-4/5/6 (and combination with Run-1/2/3)
- this presentation: Run-4/5/6 analysis and combination with previous results

FNAL Muon $g-2$ collaboration

176 collaborators, 34 institutes, 7 countries

Particle-, Nuclear-, Atomic-, Optical-, Accelerator-,
and Theoretical-Physicists and Engineers

[some faces at unblinding meeting of 20 May 2025, by P.Winter, CERN, Jun 2025]

Muon g-2 measurement technique

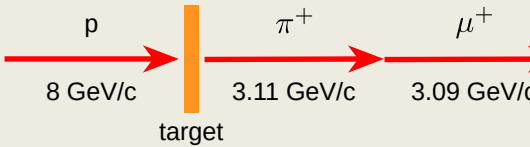

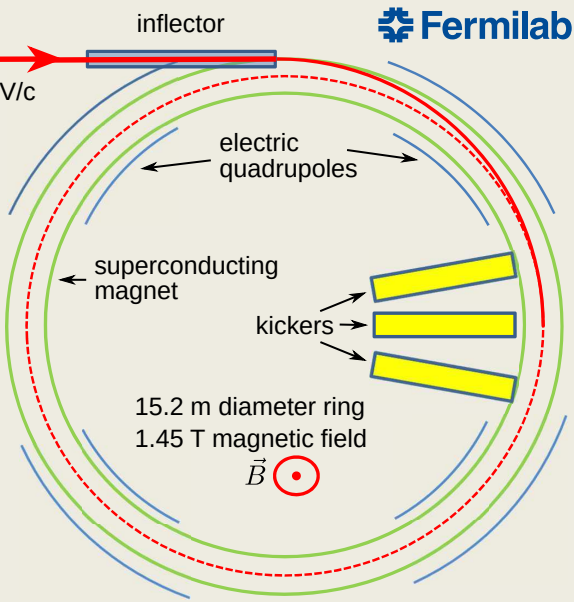

measurement principles

- store polarized muons in magnetic ring
- measure ω_a, muon spin precession
- measure ω_p, proton spin precession
  (measure average magnetic field with NMR)
- $a_\mu = \frac{\omega_a}{\omega_p} \frac{\mu_p}{\mu_B} \frac{m_\mu}{m_e}$
- precision goal 140 ppb
  (100 stat ω_a, 70 syst ω_a, 70 syst ω_p)

main improvements

- more and more pure muons than BNL

Muon g-2 measurement technique, additional details

- accounting for vertical-focusing electric field and vertical muon beam oscillations:

$$\vec{\omega}_a \equiv \vec{\omega}_s - \vec{\omega}_c = \frac{e}{m_\mu c}\left[a_\mu \vec{B} - \left(a_\mu - \left[\frac{m_\mu c}{p}\right]^2\right)\vec{\beta}\times\vec{E} - a_\mu\left(\frac{\gamma}{\gamma+1}\right)(\vec{\beta}\cdot\vec{B})\vec{\beta}\right]$$

- zero $\vec{\beta}\times\vec{E}$ term $\Rightarrow$ $p_{\text{magic}} = \dfrac{m_\mu c}{\sqrt{a_\mu}} \approx 3.094\,\text{GeV}/c$, Lorentz $\gamma_{\text{magic}} \approx 29.3$

- muon spin precession $\omega_s \approx g_\mu \dfrac{eB}{2m_\mu c} + (1-\gamma)\dfrac{eB}{\gamma m_\mu c} \approx 2\pi \cdot 6.9\,\text{MHz}$

  muon cyclotron $\omega_c \approx \dfrac{eB}{\gamma m_\mu c} \approx 2\pi \cdot 6.7\,\text{MHz}$

  muon anomalous precession $\omega_a \approx a_\mu \dfrac{eB}{m_\mu c} \approx 2\pi \cdot 229\,\text{kHz}$

  proton spin precession $\omega_p'(T) \approx g_p'(T)\dfrac{eB}{2m_p c} \approx 2\pi \cdot 61.8\,\text{MHz}$

- ω_a independent (not directly dependent) of uncertainty on muon momentum / γ

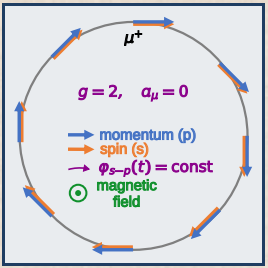

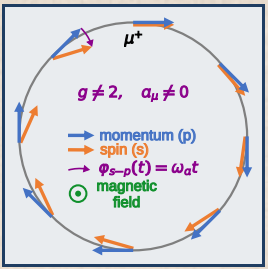

- ∼5000 stored muons per fill, 12 Hz fills
- ∼500 high-energy positrons detected per fill
- ∼310 billion analyzed high-energy positrons from muon-decays

Production of polarized muons

- dump 8 GeV protons on target to produce pions
- select pions with momemtum $p \simeq 3.11$ GeV
- let them decay into muons
- in pion rest frame, parity violation in pion decay causes μ^+ spin anti-aligned to momentum vector
- in laboratory frame, highest energy muons are >90% polarized

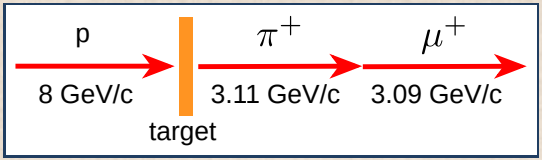

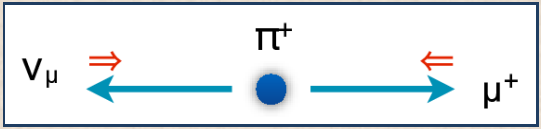

- with 8 GeV protons on target, μ^+ are produced more frequently than μ^-

Rate of high-energy muon-decay electrons modulated with $\cos \omega_a t$

- because of parity violation in muon decay, decay electrons peak along muon spin

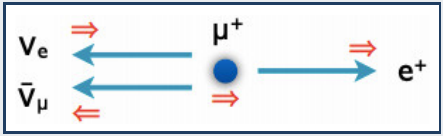

- electrons decaying along muon momentum have highest energy in laboratory frame
- $N_e(E_e > E_t) = N_{e0} e^{-t/\tau_\mu}(1 + A \cos \omega_a t)$

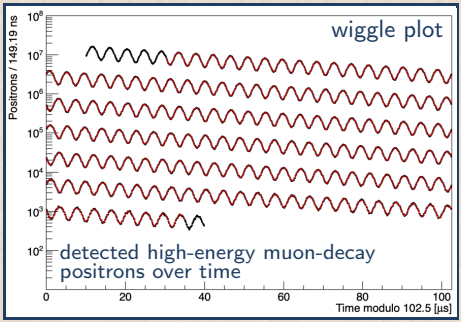

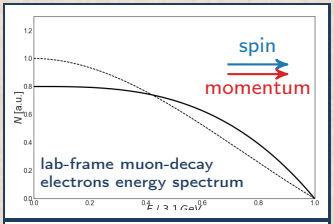

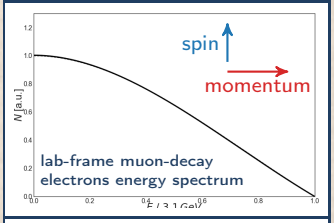

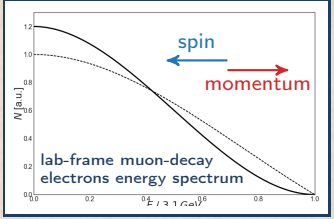

FNAL accelerator complex for Muon $g-2$

section of muon g-2 storage ring magnet

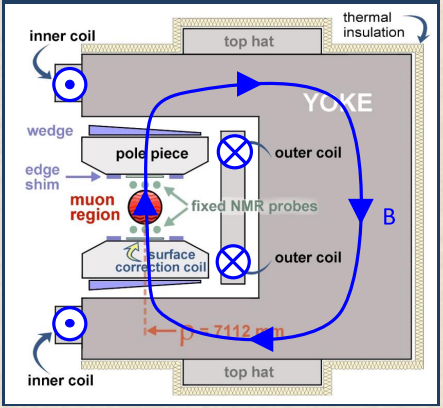

Pulsed inflector magnet injects muons into storage ring

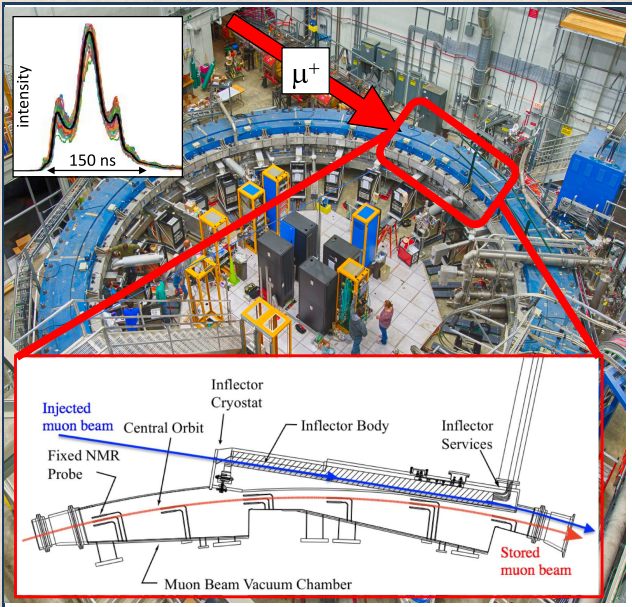

- cancels 1.45 T field in beam channel
- minimal perturbation of magnetic field in muon storage volume

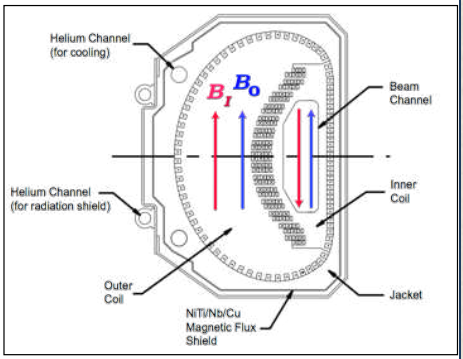

Magnetic kickers put muons into correct orbit

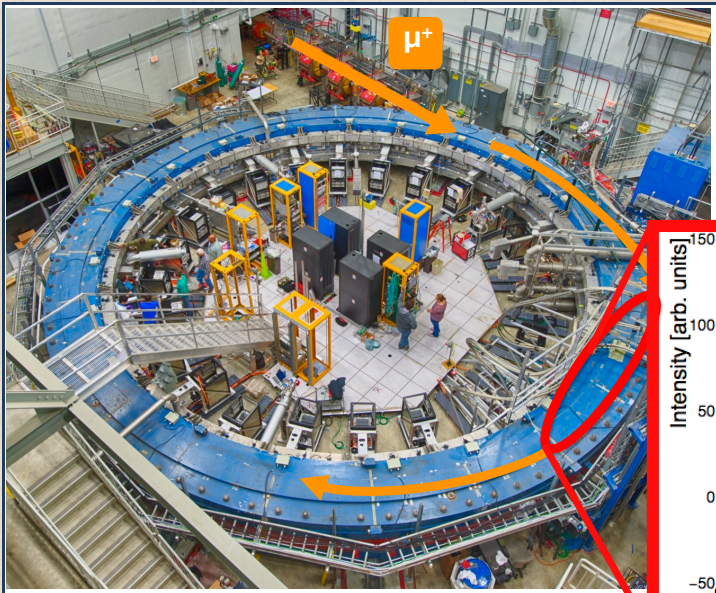

- 3 pulsed electro-magnets
- $\sim$220 G magnetic field
- $3-4$ kA peak current
- $\sim$130 ns pulse duration, shorter than cyclotron period (149.2 ns)

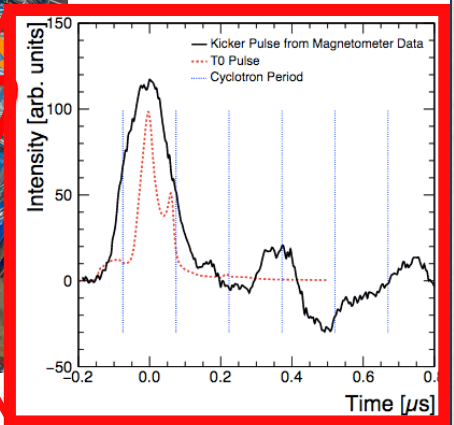

Electric quadrupoles focus beam vertically

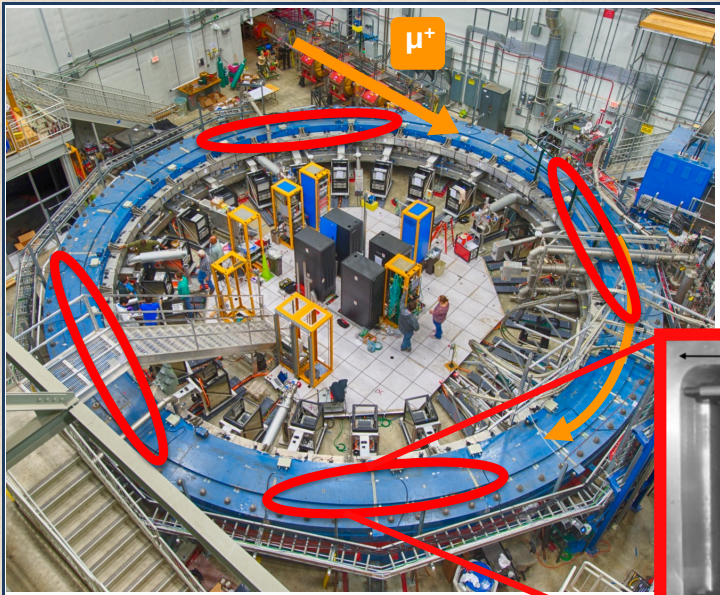

- operated in $\pm 15 - 21\,\mathrm{kV}$ range
- pulsed to avoid spatial charge accumulation

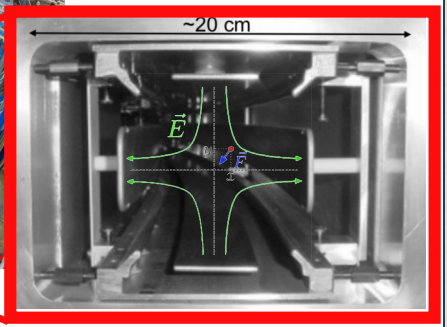

RF on quad HV to dampen radial & vertical beam dynamics

New on Run 4/5/6

- ∼1 KV radio-frequency modulation of quad high voltage in first 6 μs of quad activation during fills
  - obtained significant reduction of radial & vertical motion of average muon distribution
  - ∼10× ω_a bias reduction when not accounting for beam dynamics

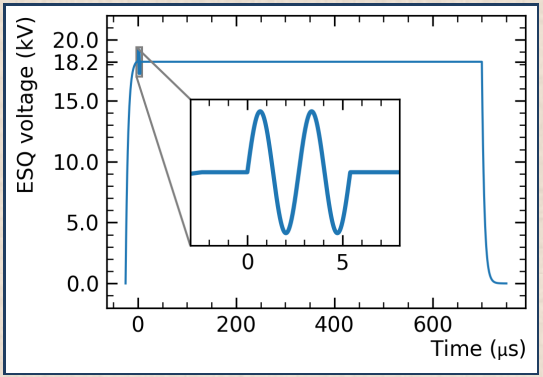

four datasets with different RF damping

- NoRF - no RF
- xRF - RF for radial (x) beam motion
- xyRF5 - RF for radial & vertical beam motion, Run 5
- xyRF6 - RF for radial & vertical beam motion, Run 6

Positrons from positive-muons' decays are detected

- positrons from positive muons decays curl inward and are detected
- calorimeters measure energy for ω_a measurement
- trackers reconstruct muon decay vertices to measure beam dynamics

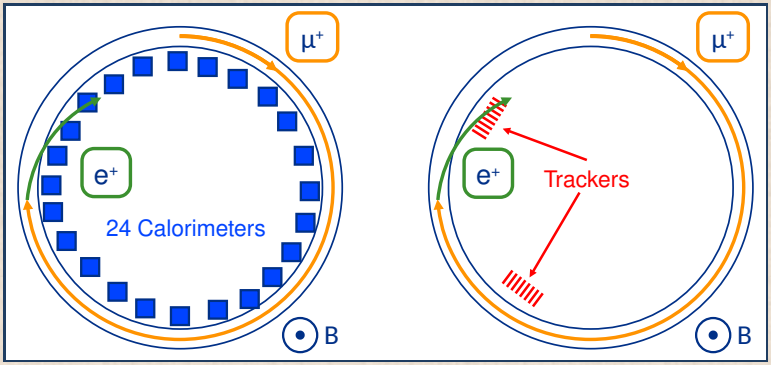

Two tracker modules

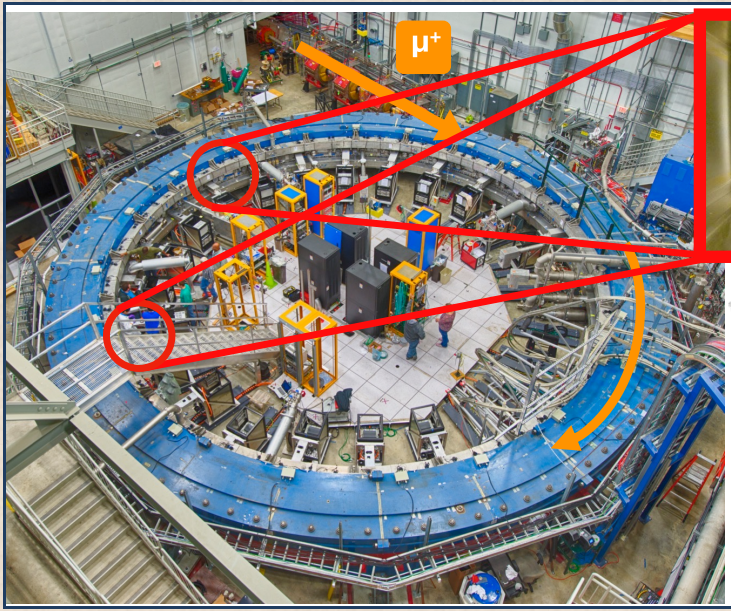

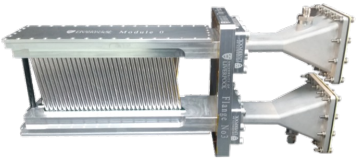

each tracker

- 8 modules
- 128 straw chambers each
- trace back muon decay points

24 calorimeter modules

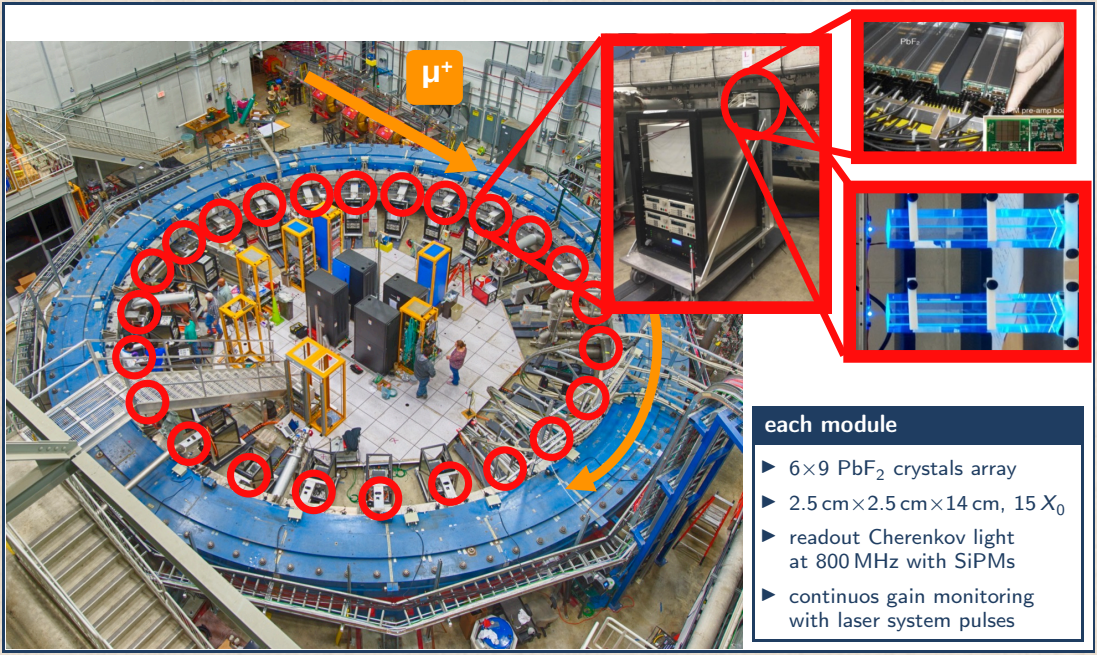

each module

- 6×9 PbF_2 crystals array
- $2.5\,\text{cm} \times 2.5\,\text{cm} \times 14\,\text{cm}$, $15\,X_0$
- readout Cherenkov light at 800 MHz with SiPMs
- continuos gain monitoring with laser system pulses

Laser calorimeter gain monitoring system

- SiPM gain is reduced by occurrence of preceding hits
- if unaccounted, sizeable bias on ω_a measurement
- gain monitored by reading back reference laser light pulses injected in calorimeter PbF_2 crystals
  - also during data-taking
- positron energy measurement from SiPM readout corrected for average measured gain loss

μs time scale SiPM power supply recovery time

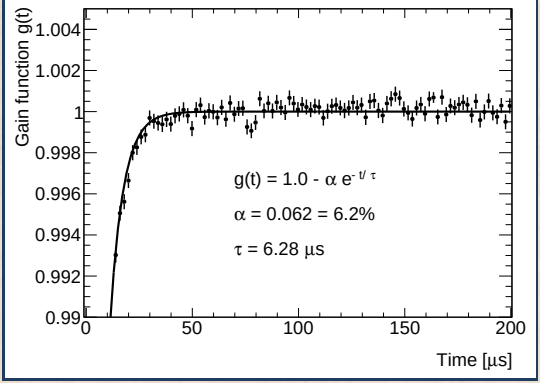

ns time scale SiPM pixel recovery time

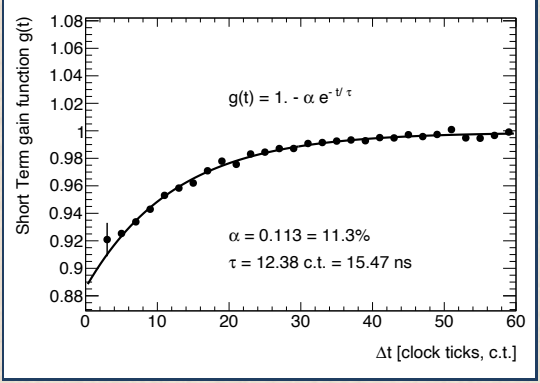

ω_a^m wiggle plot fit, 5 parameters function

$$N(t) = N_0 e^{-t/\tau_\mu} [1 + A\cos(\omega_a t + \varphi)]$$

- $N(t)$: number of e^+ vs. time
- N_0: normalization
- τ_μ: dilated μ^+ lifetime
- A: wiggle asymmetry
- ω_a: anomalous precession frequency
- φ: average spin phase at injection

- peaks in Fourier transform of fit residuals
- biases of order 1 ppm

wiggle plot

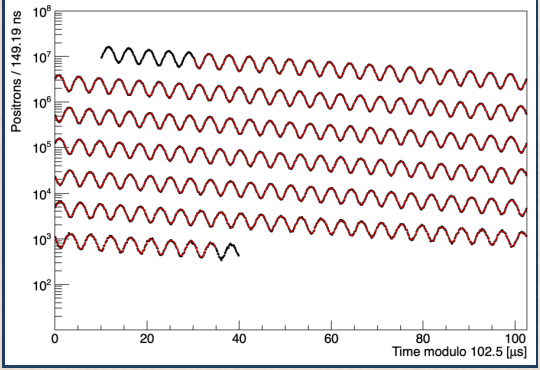

Fourier transform of wiggle plot fit residuals

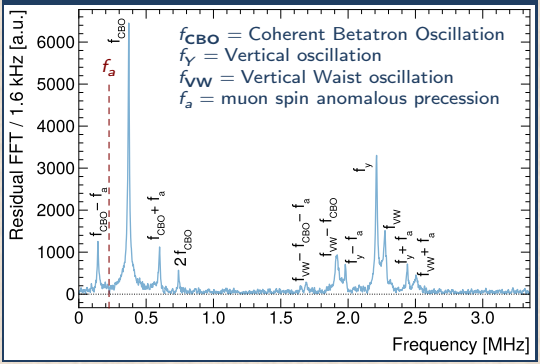

ω_a^m wiggle plot fit, full function

- ∼30-parameter typical fit function to account for
  - beam vertical and horizontal/radial motion
  - muon loss
- no peaks in Fourier transform of fit residuals
- good χ^2 [largest statistics dataset $\chi^2/\text{ndof} = 4007/4097$, $p = 84\%$]

example full ω_a fit function

$$N_0\, e^{-\frac{t}{\gamma\tau}}\,(1 + A \cdot A_{BO}(t)\cos(\omega_a t + \phi \cdot \phi_{BO}(t))) \cdot N_{\mathrm{CBO}}(t) \cdot N_{\mathrm{VW}}(t) \cdot N_y(t) \cdot N_{2\mathrm{CBO}}(t) \cdot J(t)$$

$$A_{\mathrm{BO}}(t) = 1 + A_A \cos(\omega_{\mathrm{CBO}}(t) + \phi_A) e^{-\frac{t}{\tau_{\mathrm{CBO}}}}$$

$$\phi_{\mathrm{BO}}(t) = 1 + A_\phi \cos(\omega_{\mathrm{CBO}}(t) + \phi_\phi) e^{-\frac{t}{\tau_{\mathrm{CBO}}}}$$

$$N_{\mathrm{CBO}}(t) = 1 + A_{\mathrm{CBO}} \cos(\omega_{\mathrm{CBO}}(t) + \phi_{\mathrm{CBO}}) e^{-\frac{t}{\tau_{\mathrm{CBO}}}}$$

$$N_{2\mathrm{CBO}}(t) = 1 + A_{2\mathrm{CBO}} \cos(2\omega_{\mathrm{CBO}}(t) + \phi_{2\mathrm{CBO}}) e^{-\frac{t}{\frac{1}{2}\tau_{\mathrm{CBO}}}}$$

$$N_{\mathrm{VW}}(t) = 1 + A_{\mathrm{VW}} \cos(\omega_{\mathrm{VW}}(t)t + \phi_{\mathrm{VW}}) e^{-\frac{t}{\tau_{\mathrm{VW}}}}$$

$$N_y(t) = 1 + A_y \cos(\omega_y(t)t + \phi_y) e^{-\frac{t}{\tau_y}}$$

$$J(t) = 1 - k_{LM} \int_{t_0}^{t} \Lambda(t) dt$$

$$\omega_{\mathrm{CBO}}(t) = \omega_0 t + A e^{-\frac{t}{\tau_A}} + B e^{-\frac{t}{\tau_B}}$$

$$\omega_y(t) = F\omega_{\mathrm{CBO}(t)}\sqrt{2\omega_c/F\omega_{\mathrm{CBO}}(t) - 1}$$

$$\omega_{\mathrm{VW}}(t) = \omega_c - 2\omega_y(t)$$

Fourier transform of wiggle plot fit residuals

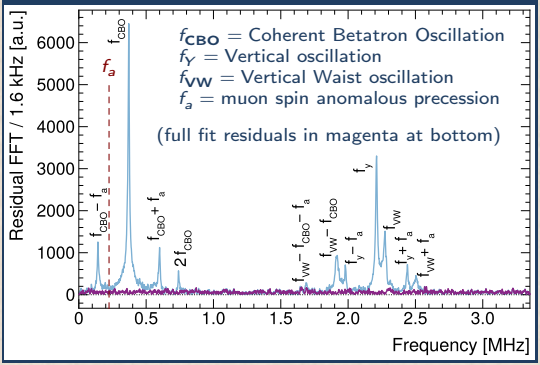

Measuring ω_a^m with ∼30 ppb systematic accuracy for Run 4/5/6

- 5 independent and mutually software-blinded analysis groups
- completed total of 20 analyses (on each of 4 Run 4/5/6 datasets)
- consistency checks of SW and HW blind analyses
- consistency checks of common-HW-blinded analyses
- to estimate statistical correlations between analyses
  - assembled 200 bootstrap samples extracting datasets subruns
  - estimated between-analyses correlations on data
  - bootstrap samples planned and performed for most analyses
    (has been done in few cases also when performing Run 2/3 measurement)

New on Run 4/5/6

- perform one analysis fit on the wiggle plot assembled for another analysis
- all these tests either succeeded or facilitated debugging and well-understood fixes

ω_a^m measurement done separately on 4 datasets

- for each dataset, ω_a^m = even average of 7 analyses using most precise methods
  - conservative 100% correlation assumed for each statistical and systematic uncertainty component
  - safe, stable, and only 1.5% larger uncertainty than optimal average

Run 4,5,6 ω_a measurements, 5 groups, 8 methods, 20 analyses

groups

g
BU
RE1
RE2
RE3
RE4
EU
Ky
SJTU

reconstructions

r
RW
RE
RI2
RQ

analyses

g	m	r	rq
BU	T, A, RT, RA	RW	K
RE1	T, A	RE	R
RE2	T, A	RE	
RE3	RT, RA	RE	R
RE4	ST, SA	RE	
EU	T, A, RT, RA	RI2	R
UK	Q, RQ	RQ	R
SJTU	T, A	RW	

measurement methods

m	method
T	Threshold
A	Asymmetry weighted
RT	Ratio T
RA	Ratio A
Q	Charge
RQ	Ratio Charge
ST	Stroboscopic T
SA	Stroboscopic A

pileup subtraction

ps
RW-BU
RE
RW-EU
RW-SJTU

ratio quartering methods

rq	ratio quartering methods
R	random
K	kernel

envelope modeling

em
analytic function
spline
Gaussian Process Regression

ω_a^m measurements must be consistent within each dataset

20 ω_a^m measurements on 4 Run 4+5+6 datasets

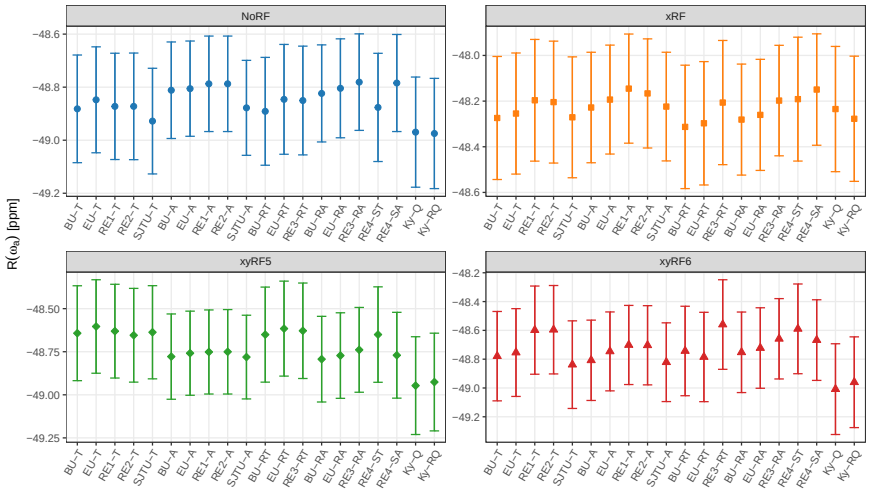

- however, statistical uncertainties within same datasets are highly correlated

ω_a^m measurements with just their systematic uncertainties' estimates

20 ω_a^m measurements on 4 Run 4+5+6 datasets

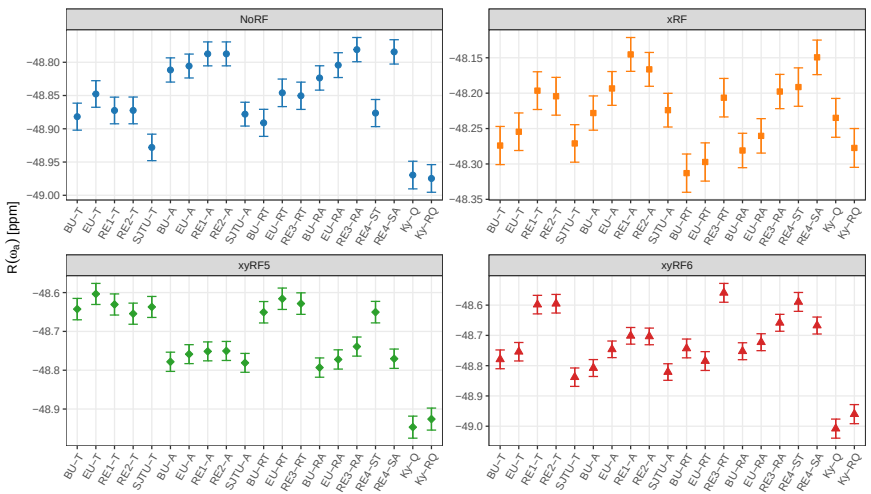

- even assuming uncorrelated systematics, ω_a^m measurements are inconsistent
- estimate variance-contributing statistical decorrelation between analyses using bootstrap samples

Pulls – dealing with analysis-group-dependent blinding offsets

- consistency checks for group-dependent blinding offsets possible relying on different datasets
- $\text{pull} = \dfrac{(\omega_a^{\text{dataset 2, analysis 2}} - \omega_a^{\text{dataset 2, analysis 1}}) - (\omega_a^{\text{dataset 1, analysis 2}} - \omega_a^{\text{dataset 1, analysis 1}})}{\sqrt{\sigma^2(\omega_a^{\text{dataset 2, analysis 2}} - \omega_a^{\text{dataset 2, analysis 1}}) + \sigma^2(\omega_a^{\text{dataset 1, analysis 2}} - \omega_a^{\text{dataset 1, analysis 1}})}}$

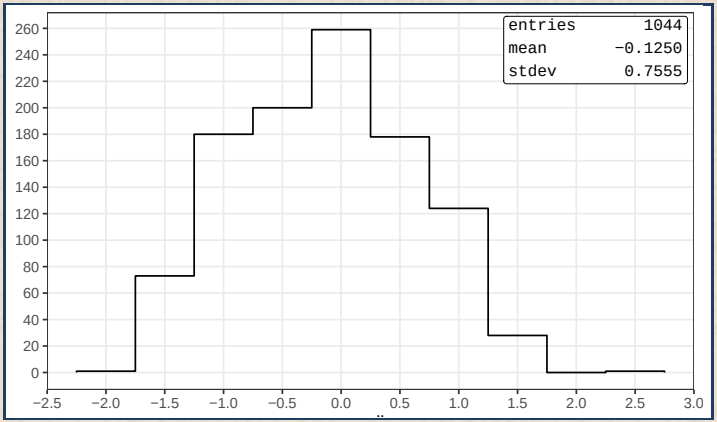

Pulls after removing group-dependent blinding offsets

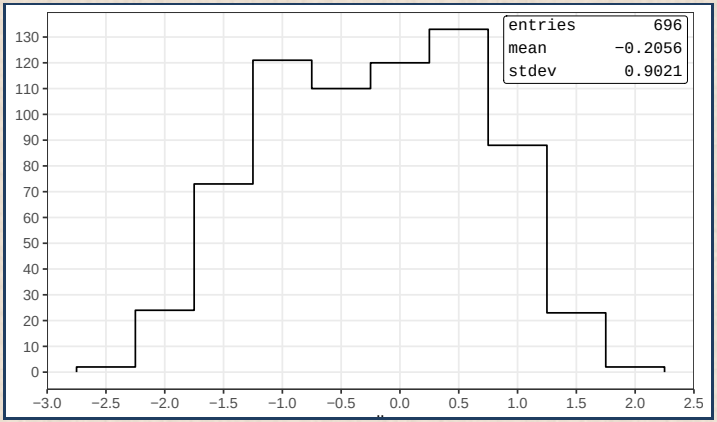

Positron-rate-dependent calorimeter gain sag

New on Run 4/5/6

- calorimeter gain sag after calorimeter hits due to SIPM power supply recovery time
  - well known, measured with laser monitoring system using high power test laser pulses
  - occurs with injection beam flash, measured with laser monitoring during data-taking, and corrected
- time-dependent rate of positron hits contributes additional gain sag over fill time
  - below sensitivity of laser monitoring system during data-taking
  - dedicated studies estimated order 40 ppb ω_a bias because of phase difference w.r.t. ω_a phase
  - confirmed with extra studies performed with laser pulses after end of data-taking
- Run 4/5/6: estimated positron gain sag bias subtracted, updated systematic uncertainty
- Run 1 & 2/3: revised published results, accounting for updated understanding

Measurement of the magnetic field map $\omega_p'(T_r)^m$

- in-vacuum trolley with NMR probes maps magnetic field every ∼3 days

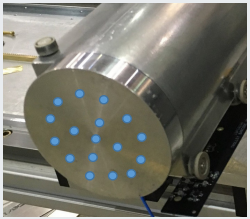

trolley with 17 probes

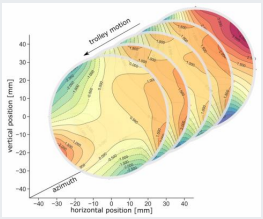

2-D field maps (∼8000 points)

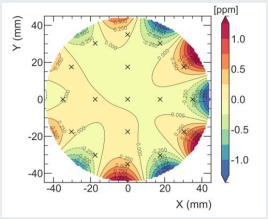

azymutally averaged field map

- 378 fixed probes monitor field during muon storage at 72 locations

Fixed probes above/below muon storage region

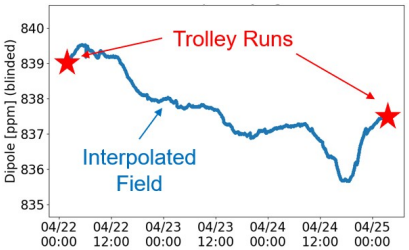

Measurement of the magnetic field, probes calibration

- calibrate petroleum-jelly trolley probes with cylindrical H_2O probe (plunging probe) in same physical positions [20 ppb consistency and reproducibility]

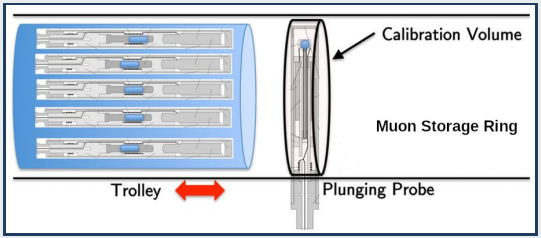

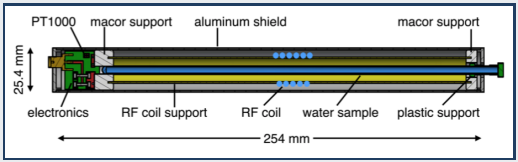

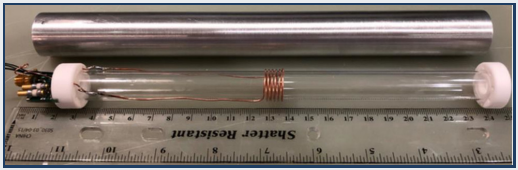

- calibrate plunging probe in ANL MRI magnet
  - reference spherical H_2O probe [15 ppb precision]
  - reference ^3He probe [20 ppb precision]

H_2O probe

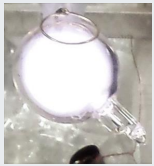

^3He probe

Measurement of the magnetic field, weighting with muon distribution map M

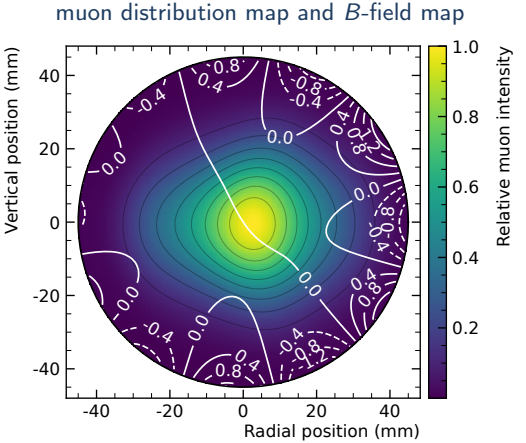

- muon distribution map M reconstructed
  - with trackers in close to trackers
  - with trackers + simulation elsewhere

- $\tilde{\omega}'_p(T_r)^m = \omega'_p(T_r)^m \times M$ B-field map weighted with muon distribution map [48 ppb precision]

Corrections to ω_a^m and $\tilde{\omega}_p'(T_r)^m$

$$R'_\mu(T) = \frac{\omega_a}{\tilde{\omega}_p'(T_r)} = \frac{\omega_a^m}{\tilde{\omega}_p'(T_r)^m} \frac{1 + C_e + C_p + C_{\text{pa}} + C_{\text{dd}} + C_{\text{ml}}}{1 + B_k + B_q}$$

corrected / measured / corrected / measured

beam-dynamics corrections

transient-fields corrections

- C_e quadrupole electric field outside magic radius
- C_p spin-precession contribution from muon vertical oscillation motion
- C_{pa} time-variation of mean muon distribution phase from detector acceptance and beam motion
- C_{dd} time-variation of mean muon distribution phase from momentum-dependent muon lifetimes
- C_{ml} time-variation of mean muon distribution phase from momentum-dependent muon storage losses
- B_k transient B-field generated by kicker eddy currents
- B_q transient B-field from vibration of plates of pulsed electrostatic quadrupole field system

E-field correction C_e: largest one & largest systematic contribution

depends on radial muon distribution,
equivalent to momentum distribution,
obtained with three detectors:

- calorimeters
  - parasitic on data-taking
  - measure injected muon bunches dephasing (how muons spread along the beam over time)
  - improved elaborations

  New on Run 4/5/6
- trackers
  - parasitic on data-taking
  - complement with beam dynamics simulation
  - measure muon radial distribution along ring
- Miniscifi (Minimally Intrusive Scintillating Fiber detector)

  New on Run 4/5/6
  - dedicated runs
  - complement with beam dynamics simulation
  - measure muon radial distribution

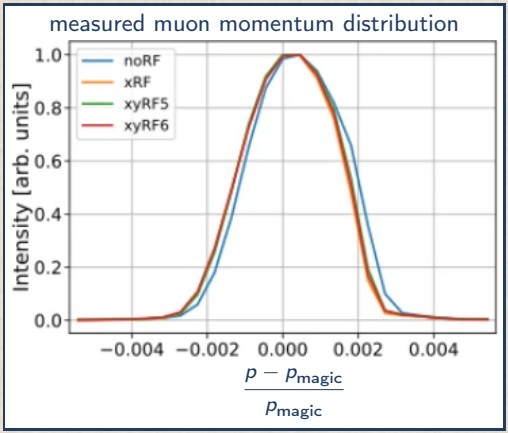

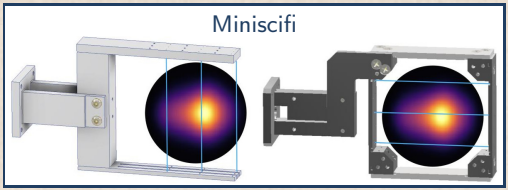

E-field correction C_e: largest one & largest systematic contribution

- using 3 different consistent approaches $\Rightarrow$ systematic uncertainty reduced to 27 ppb

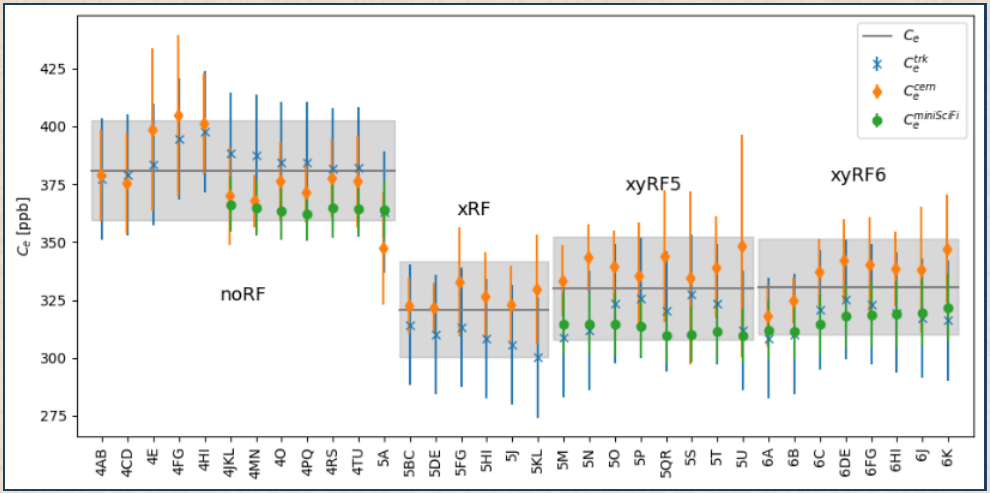

Kicker transient field measured with two magnetometers

New on Run 4/5/6

- measure Faraday rotation of polarized laser light in TGG crystal
- two independent teams and detectors
- higher transient field measured off magic-radius
- ckecks with hardware mockup
- -37 ± 22 ppb correction to B-field
- Run 1 & 2/3 results revised with improved understanding

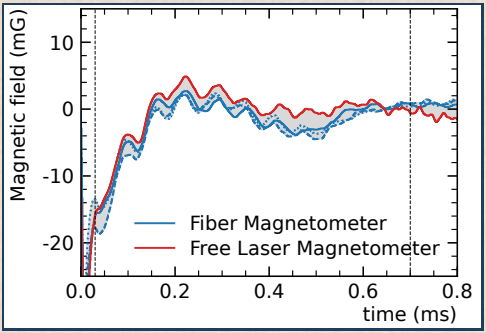

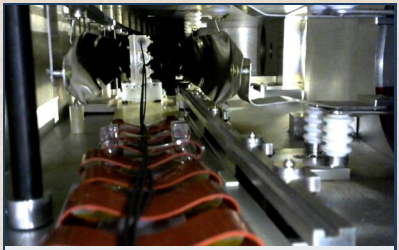

fiber magnetometer

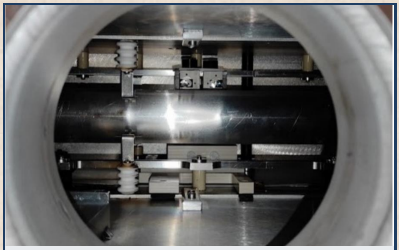

free laser magnetometer

Systematic corrections and uncertainties for Run 4/5/6

Quantity	Correction (ppb)	Uncertainty (ppb)
ω_a^m (statistical)	···	114
ω_a^m (systematic)	···	30
C_e	347	27
C_p	175	9
C_{pa}	-33	15
C_{dd}	26	27
C_{ml}	0	2
$\omega_p'(T_r)^m$ (mapping, tracking)	···	34
$\omega_p'(T_r)^m$ (calibration)	···	34
B_k	-37	22
B_q	-21	20
$\mu_p'(T_r)/\mu_B$	···	4
m_μ/m_e	···	22
Total systematic for $R_\mu'(T_r)$	···	76
Total for a_μ	572	139

$$a_\mu = \frac{\omega_a}{\tilde{\omega}_p'(T_r)} \frac{\mu_p'(\mathrm{Tr})}{\mu_B} \frac{m_\mu}{m_e}$$

- external inputs from CODATA 2022
- $T_r = 25\,^\circ\mathrm{C}$

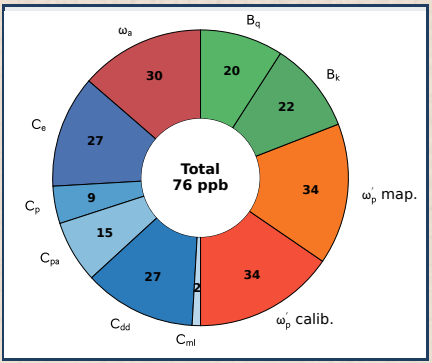

- total systematic < 100 ppb (design)
- systematics evenly distributed

Result

- results blinded by unknown offset in calorimeter DAQ sampling frequency
- collaboration approved result before unblinding on 20 May 2025
- BNL, FNAL Run 1 & 2/3 $R'_\mu(T_r)$, $\omega'_p(T_r)$ converted to spherical water sample at $T_r = 25\,^\circ\text{C}$
- FNAL Run 1 & 2/3 results revised
- experimental results on $R'_\mu(T_r)$ have been combined (100% correlated systematics for FNAL measurements)
- PRL 135 (2025) 101802

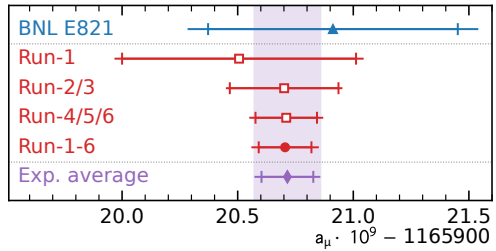

a_μ FNAL $= 0.001165920705\ (148)\ [127\ \text{ppb}]$
a_μ EXP $= 0.001165920715\ (145)\ [124\ \text{ppb}]$

$R'_\mu(T_r)$	uncertainty stat. [ppb]	syst. [ppb]	total [ppb]
Run-1	434	159*	462
Run-2/3	201	78*	216
Run-4/5/6	114	76	137
Run-1-6	98	78	125

*revised

Result

- results blinded by unknown offset in calorimeter DAQ sampling frequency
- collaboration approved result before unblinding on 20 May 2025
- BNL, FNAL Run 1 & 2/3 $R'_\mu(T_r)$, $\omega'_p(T_r)$ converted to spherical water sample at $T_r = 25\,^\circ\mathrm{C}$
- FNAL Run 1 & 2/3 results revised
- experimental results on $R'_\mu(T_r)$ have been combined (100% correlated systematics for FNAL measurements)
- PRL 135 (2025) 101802

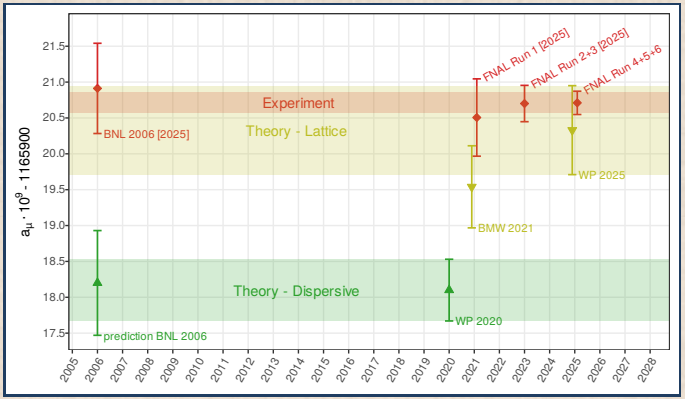

$R'_\mu(T_r)$	uncertainty stat. [ppb]	syst. [ppb]	total [ppb]
Run-1	434	159*	462
Run-2/3	201	78*	216
Run-4/5/6	114	76	137
Run-1-6	98	78	125

*revised

Consistency of Run 4/5/6 datasets, ω_a vs. $\tilde{\omega}'_p(T_r)$

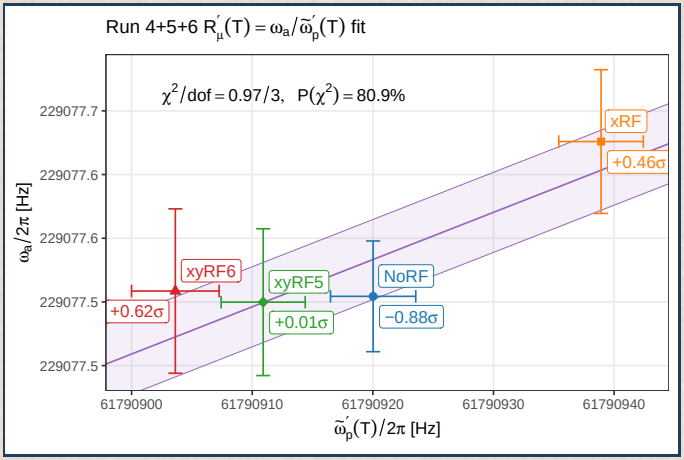

Finer (blind) Consistency of Run 4/5/6 datasets, $R'_\mu(T_r) = \omega_a$ vs. $\tilde{\omega}'_p(T_r)$

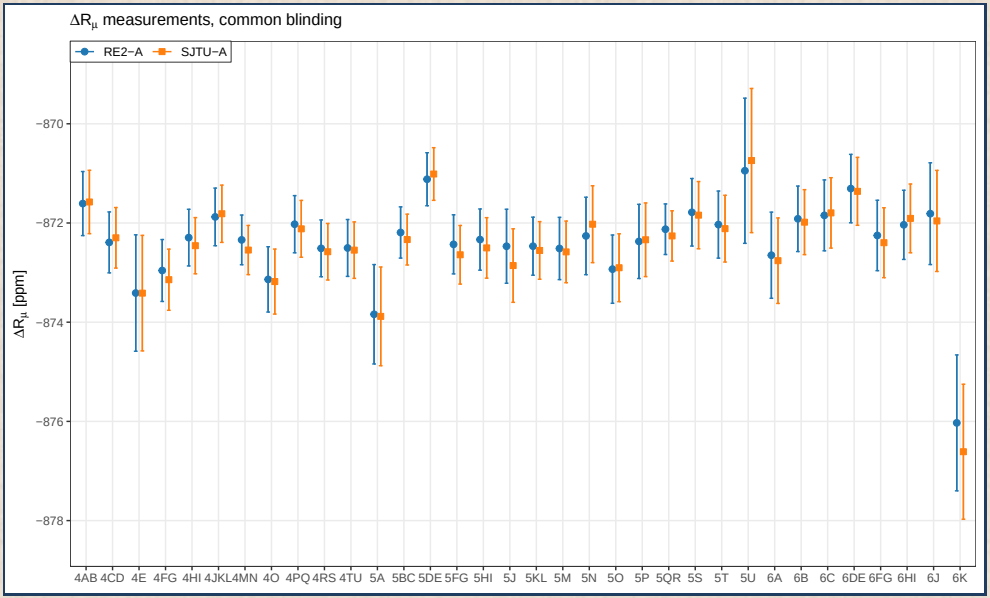

Consistency of BNL final report and FNAL datasets

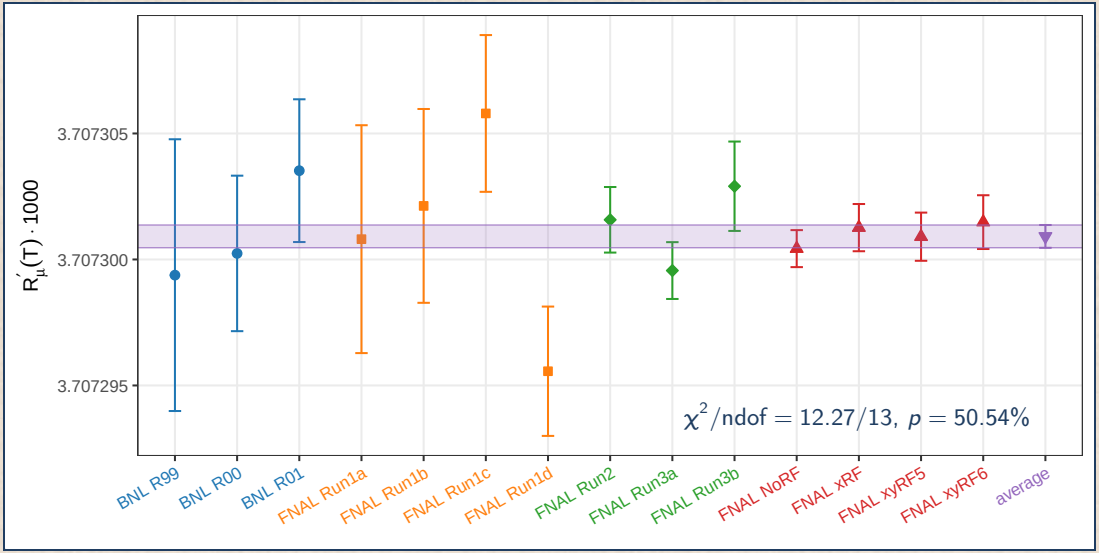

Consistency of BNL final report and FNAL datasets, ω_a vs. $\tilde{\omega}'_p(T_r)$

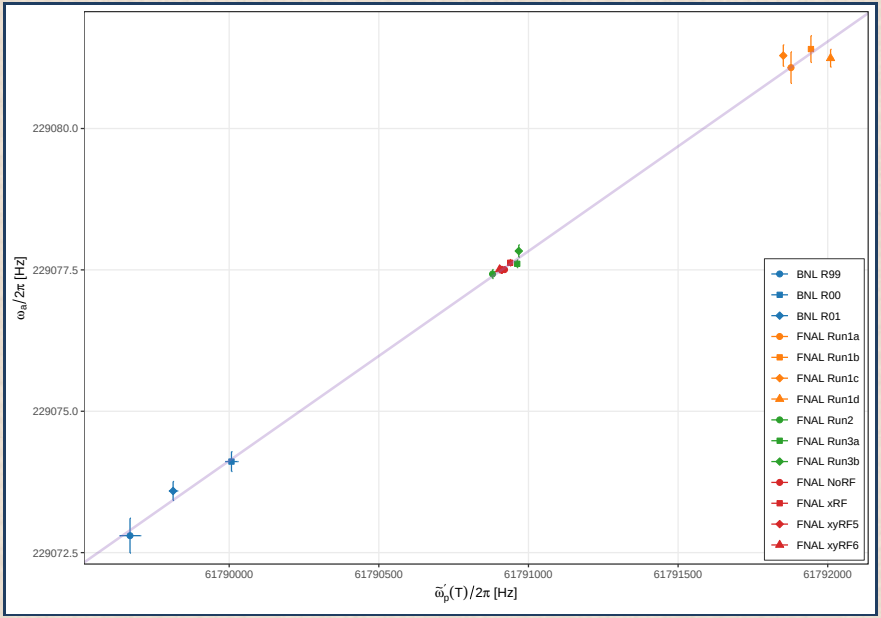

Conclusion

- most precise a_μ measurement for many years to come
- key ingredient of SM test
- tight constraint on New Physics models

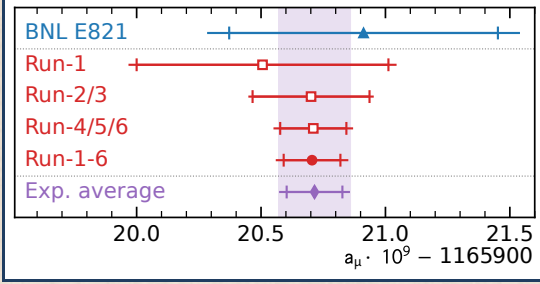

PRL 135 (2025) 101802

Backup slides

Pileup

- get pileup correction from data
  count hits in test window close to each existing hit
- series of improvements in Run 2/3 and Run 4/5/6
  - better reconstruction ⇒ reduced pileup hits
  - apply modeling of pileup built from real data hits
- estimated pielup statistically subtracted

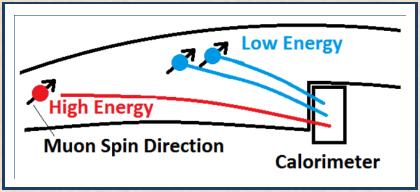

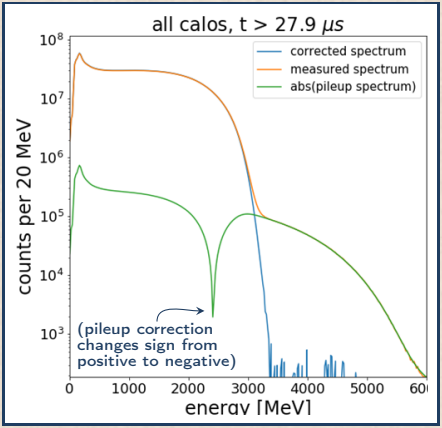

reduced pileup in Run 2+3

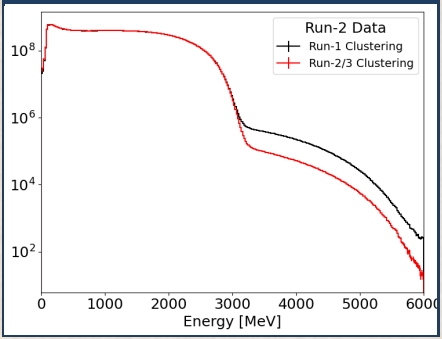

Use data bootstrap samples to estimate ω_a^m measurements correlation

- for each dataset, build 200 bootstrap samples of same size
  by ramdomly selecting DAQ subruns, with repetitions [B. Efron, Annals Statist. 7 (1979)]
  (subruns are DAQ files, each containing around 37 K muon decays with energetic positrons in the calorimeters)
- for each analisys i, perform fits on 200 bootstrap samples $\Rightarrow$ ω_a^m fit measurements $m_{i,b}$
- estimate ω_a^m covariance: $\mathrm{cov}(m_1, m_2) = \dfrac{\sum_b (m_{1,b} - \overline{m}_1)(m_{2,b} - \overline{m}_2)}{N_b - 1}$ with $\overline{m}_i = \dfrac{\sum_b m_{i,b}}{N_b}$
- expected residual uncertainty $\sigma^2 (m_2 - m_1) = \sigma_1^2 + \sigma_2^2 - 2\rho\sigma_1\sigma_2$

bootstrap samples produced for most analyses

group	method	RF datasets
BU	T, A, RT, RA	No, x, xy5, xy6
EU	T, A, RT, RA	No, x, xy5, xy6
RE1	T, A	No, x, xy5, xy6
RE2	T, A	No, x, xy5, xy6
RE3	RA	No, x, xy5, xy6
RE4	SA	No, x, xy5, xy6
SJTU	T, A	No, x, xy5, xy6

correlations between Q-x vs. A-x & T-x analyses

- bootstrap samples fits not done for Q-x analyses
- reliable correlation evaluations using
  fits on 34 sub-samples of Run 4+5+6 sample

past evaluations of analyses' correlations

- used for checks and addition some alternative evaluations of analyses' correlations from past dedicated studies done, for Run 2+3 measurement (partly outdated)

Bootstrap ω_a^m distribution width consistent with fit uncertainty

trimmed bootstrap ω_a^m distribution

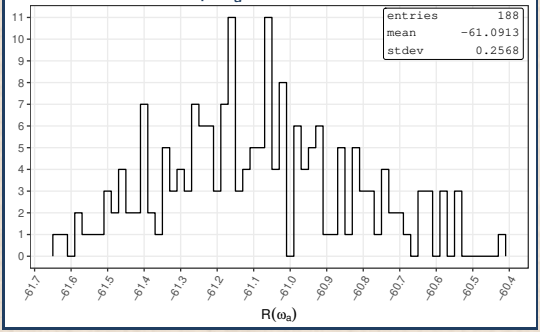

- removed $>3\,\sigma$ outliers of $m_{i,b}$ distribution

bootstrap RMS width / ω_a^m fit uncertainty

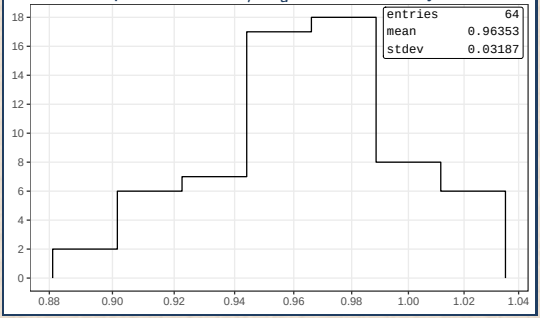

- bootstrap ω_a^m RMS width consistent with ω_a^m fit uncertainty when taking into account $3\,\sigma$ trimming

Residual uncertainties

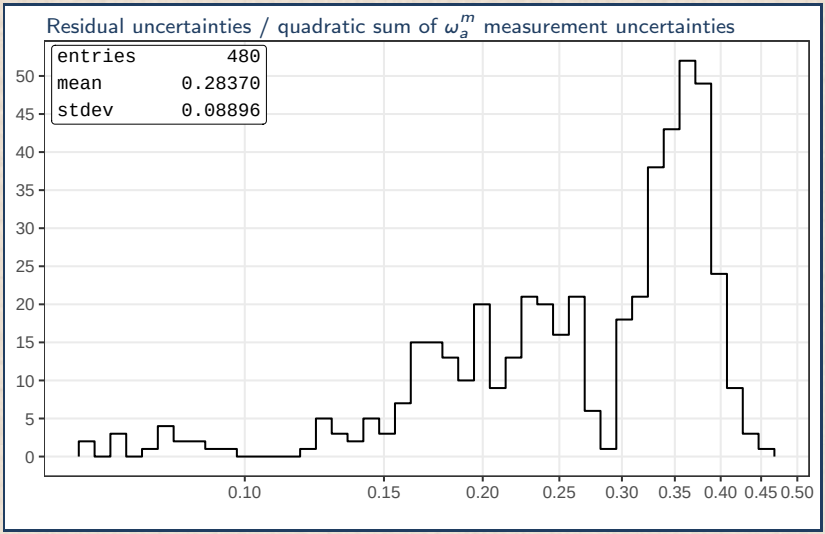

- large uncertainties: different methods (Q-A, Q-T, A-T)
- small uncertainties: ratio vs. non-ratio, different reconstructions

Beam dynamics frequencies

			f [MHz]	T [μs]
Anomalous precession	f_a		0.2291	4.3649
Cyclotron	f_c		6.7024	0.1492
Horizontal betatron	f_x	$= f_c\sqrt{1-n}$	6.2874	0.1590
Vertical betatron	f_y	$= f_c \cdot \sqrt{n}$	2.3218	0.4307
Coherent betatron oscillation	f_{CBO}	$= f_c - 1 \cdot fx$	0.4150	2.4097
Vertical oscillation	f_{VO}	$= f_c - 1 \cdot fy$	4.3806	0.2283
Vertical waist	f_{VW}	$= f_c - 2 \cdot fy$	2.0589	0.4857

typical field index $n = 0.12$

Coherent Betatron Oscillation

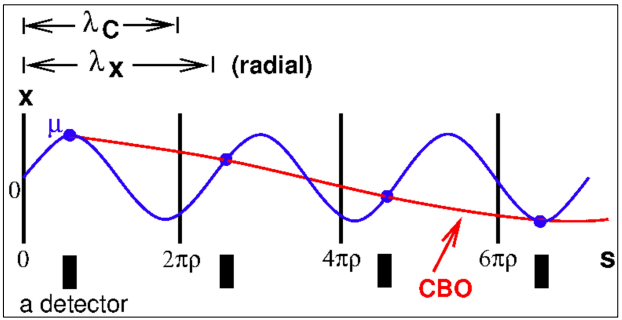

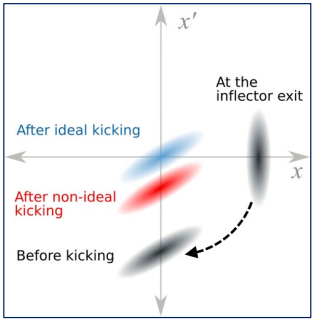

- Calo acceptance depends on muon radius at decay: coherent beam motion modulates e^+ time spectrum
- Radial betatron wavelength (blue line) $\neq$ circumference (cyclotron wavelength)
- Red line: apparent radial breathing in and out of beam at alias frequency $f_{\text{CBO}} = f_{\text{cyclotron}} - f_{\text{betatron}}$
- Effect dephases gradually, nearly cancels when all detectors added together

[D.Kawall, Sep 2023]

Absolute Field Measurement with Pulsed NMR

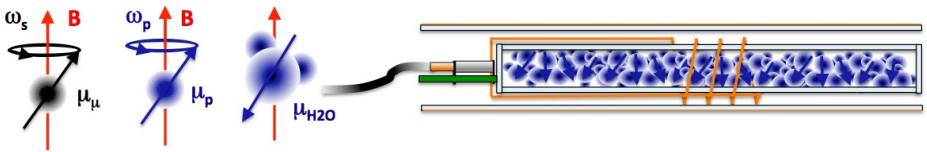

$$\omega_p'(T_R) \;=\; \omega_p^{\text{probe}} \left[1 + \frac{1}{\gamma_p'}\frac{d\gamma_p'}{dT}(T - T_R) + \left(\epsilon - \frac{4\pi}{3}\right)\chi_{\text{H}_2\text{0}}(T) \;+\; \delta_{\text{materials}}\right]$$

⇒ Determine B seen by muons from measurement of ω_p' of protons in spherical H_2O sample

- Complication: Diamagnetic shielding of electrons screens protons, *changes local* B, is T dependent, 10.36 ppb/C
- Complication: Very hard to make a spherical water sample
- Complication: magnetic susceptibility $\chi_{H_2O} \approx -0.721(2) \times 10^{-6}$ of water sample gives shape-dependent field perturbation: $\epsilon = 4\pi/3$ for a sphere, $\epsilon = 2\pi$ for cylinder $_\perp \vec{B}$, 1.5 ppm shift !!!
- Complication: Best measurement of $\chi_{\text{H}_2\text{O}}$ comes from 1933! Working on update
- Complication: Magnetization of probe materials further perturbs field at site of protons

⇒ Determine total correction to 15 ppb accuracy or better using special calibration probes

[D.Kawall, Sep 2023]

Pitch correction

- proportional to vertical muon velocity component (parallel to magnetic field)
- obtained using vertical spatial distribution of muons, measured by trackers

vertical decay vertices distribution

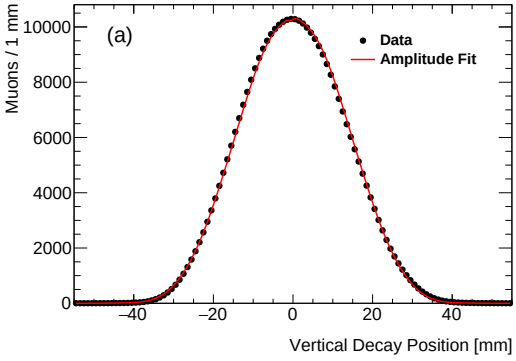

vertical oscillation amplitude distribution

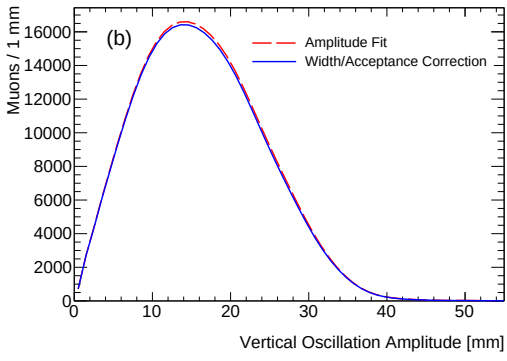

Phase changes over each fill

example: phase variation due to muon loss

- $N(t) = N_0 e^{-t/\tau_\mu} [1 + A\cos(\omega_a t + \varphi)]$ phase φ = muon spin-momentum angle at injection
- muon loss depends on momentum $\Rightarrow$ muon sample momentum varies $\bar{p} = \bar{p}(t)$
- single muon phase depends on momentum (because of production chain) $\bar{\varphi} = \bar{\varphi}(\bar{p})$
- at first order $\bar{\varphi}(t) = \bar{\varphi}_0 + \frac{d\bar{\varphi}}{dt} t = \bar{\varphi}_0 + \frac{d\bar{\varphi}}{d\bar{p}} \frac{d\bar{p}}{dt} t \simeq \bar{\varphi}_0 + \bar{\varphi}' t$
- muon rate modulation $\cos(\omega_a t + \bar{\varphi}(t)) \simeq \cos(\omega_a t + \bar{\varphi}_0 + \bar{\varphi}' t) = \cos[(\omega_a + \bar{\varphi}')t + \bar{\varphi}_0]$
  $\Rightarrow \Delta\omega_a = \bar{\varphi}'$
- note: muon loss phase effect is different and additional to muon loss effect on positron rate

Phase-Acceptance correction

- effective phase variation due to variation of beam horizontal and vertical position and spread
- example: $\Delta\omega_a = \frac{d\varphi}{dt} = \frac{d\varphi}{dY_{RMS}} \cdot \frac{dY_{RMS}}{dt}$
- obtained with simulation
- measured with trackers and extrapolated to whole ring with beam dynamics simulations

phase as a function of muon position

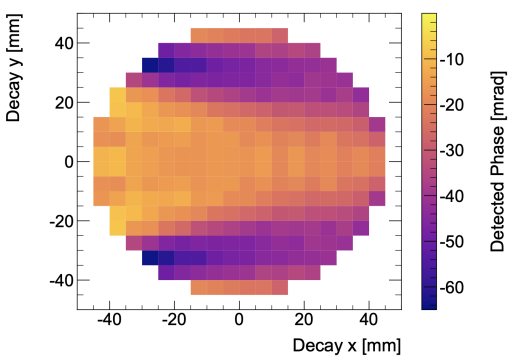

variation of Y_{RMS}

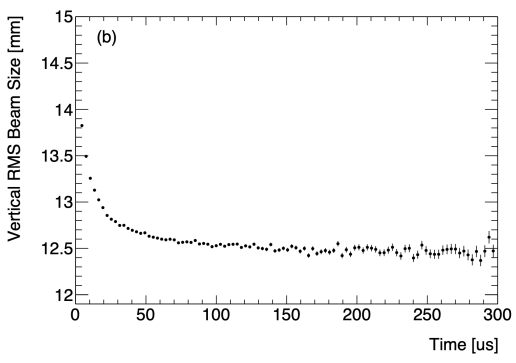

Differential decay corrections

- at $t = 0$, injected muons momentum distributoin with some average and spread
- at $t > 0$, average momentum increases because slower muons decay earlier
- phase change in fill due to variables correlated with momentum
  - horizontal displacement and velocity (x, x')
  - vertical displacement and velocity (y, y') (this is negiglible)
  - time of flight from when muon polarization is selected to kicker hit
  - momentum itself

Lost muons phase-variation effect correction

measured and simulated $\varphi - p$ correlation

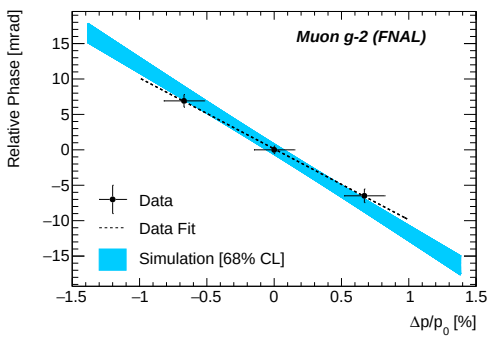

- muon phase depends on momentum
- muon population momentum changes because muon loss probability depends on momentum
- $d\varphi/dp$ measured on dedicated runs by varying magnetic field by -0.68%, +0.68%
- measurement consistent with simulation

estimated $\Delta\varphi(t)$ due to muon loss

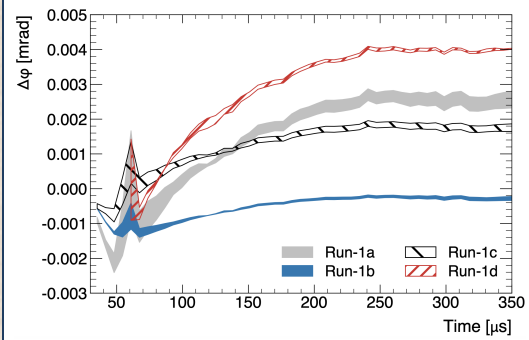

- use delivery ring collimators to change the muon momentum distribution
- muon loss function of time and momentum fitted using simulation-inspired analytic function to model observed beam loss for different muon momentum distributions

B_q correction for transient B field produced by electric quadrupoles

- electric quadrupoles are pulsed (to prevent static charge accumulation)
- conductive plates vibration perturbs magnetic field
- special NMR probes measure the transient field perturbation in muon region
- much better measured in Runs 2+ vs. Run 1

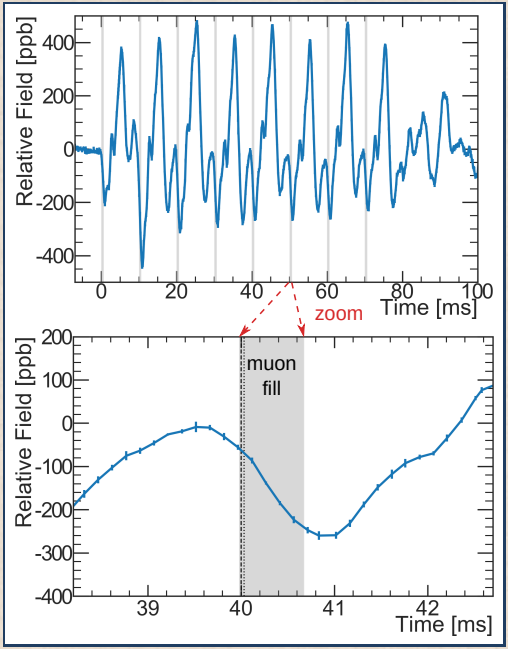

Revision from Run 2/3 to 4/5/6

before Run 4/5/6 revisions to Run 1 and Run 2/3

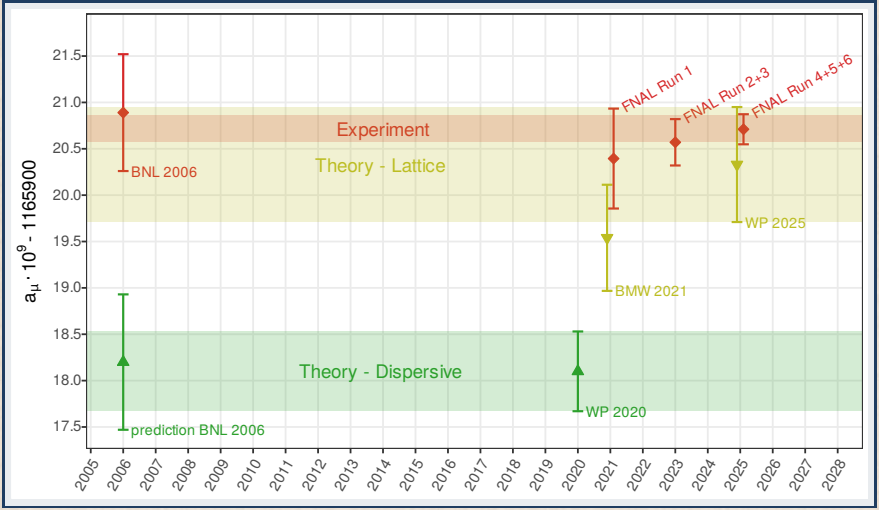

Revision from Run 2/3 to 4/5/6

after revisions